Fig. 2 (A–F) Age- and CAG-dependent changes in motor and sensory amplitudes in SBMA. CMAPs and SNAPs in the median (A and B), ulnar (C and D), tibial (E) and sural (F) nerves in different age groups are shown. The white columns are the mean values of the patients with a shorter CAG repeat (<47), while the black columns are the mean values of the patients with a longer CAG repeat (≥47). The error bars are SD. The number of patients examined is shown above each column. The young patients with a longer CAG repeat showed significantly low values of CMAPs compared to those with a shorter CAG repeat. Conversely, young patients with a shorter CAG repeat showed significantly lower values of SNAPs than those with a longer CAG repeat. Patients more than 49 years old did not show a significant difference between shorter and longer CAG repeat.

function has been reported (Doyu et al., 1992; Atsuta et al., 2006), but a CAG size-dependent clinical phenotype has not been described. This may be because the expansion of CAG repeat in the AR gene is shorter than that in the causative genes for DRPLA, SCA7 or HD. Alternatively, as compared to outstanding motor dysfunction, the clinical manifestations of sensory nerve impairment are less severe in SBMA patients, which may result in overlooking the motor and
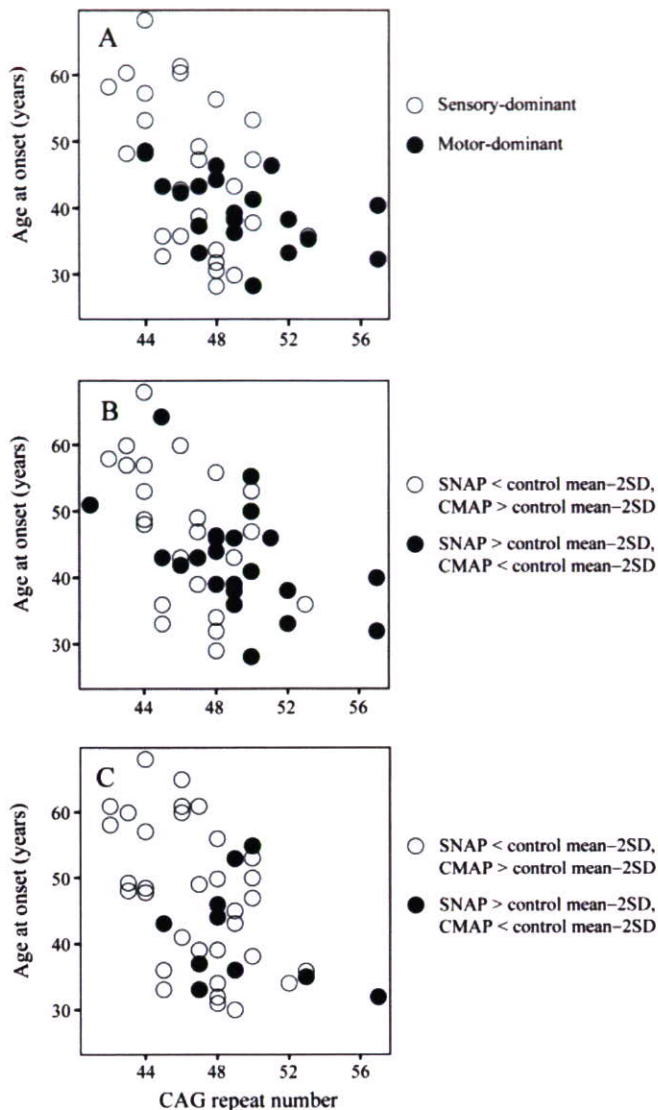
Fig. 3 CAG repeat size determines the age at onset in SBMA.
(**A**) Relation between the CAG repeat size and the age at onset
according to the phenotypes determined by CMAPs and SNAPs.
A longer CAG repeat was closely linked to the motor-dominant
phenotype, and a shorter CAG repeat was closely linked to the
sensory-dominant phenotype. Motor- and sensory-phenotypes
were determined as shown in Fig. IA. (**B**) Relation between the
CAG repeat size and the age at onset according to the phenotype
determined by using CMAPs and SNAPs in the median nerve.
(**C**) Relation between the CAG repeat size and the age at onset
according to the phenotype determined by using CMAPs and
SNAPs in the ulnar nerve.

sensory discrepancy. Our present findings in SBMA patients
strongly suggest that the phenotypic diversity determined
by CAG repeat size is a common feature shared by various
polyglutamine diseases.

Although the pathological mechanism by which CAG
repeat size influences clinical phenotype is unknown, a
common molecular basis appears to underlie the hetero-
geneity of clinical presentations in polyglutamine diseases.

The polyglutamine tract encoded by an expanded CAG
repeat forms a β-sheet structure, leading to conformational
changes and the eventual accumulation of causative
proteins (Perutz et al., 2002; Sakahira et al., 2002). Since
the propensity of aggregation is dependent on CAG repeat
size, the different length of polyglutamine tract may result
in a CAG repeat size-dependent pathology.

The observations that a longer CAG repeat results in the
motor-dominant phenotype, while a shorter CAG leads to
the sensory-dominant presentation, are further reinforced
by results of previous studies on the cell-specific histo-
pathological changes in SBMA. A diffuse loss and atrophy
of anterior horn cells accompanied by a mild gliosis is
characteristic of SBMA (Kennedy et al., 1968; Sobue et al.,
1989), suggesting that the pathology of spinal motor
neurons is neuronopathy. On the other hand, no sub-
stantial neuronal loss in the DRG despite severe axonal loss
in the central and peripheral rami suggests that the
pathology of sensory neurons is distally accentuated
axonopathy, although the primary pathological process
may be present in the perikarya of sensory neurons (Sobue
et al., 1989; Li et al., 1995). Moreover, the accumulation of
mutant AR, a pivotal feature of SBMA pathology, is also
different in motor and sensory neurons (Adachi et al.,
2005). Mutant AR accumulates diffusely in the nucleus of
spinal motor neurons, but cytoplasmic aggregation is
predominant in sensory neurons within the DRG (Adachi
et al., 2005). The extent of diffuse nuclear accumulation of
mutant AR in motor neurons is closely related to CAG
repeat size, providing a molecular basis for the present
observations that patients with a longer CAG repeat show
a greater decrease in CMAPs. On the other hand, the results
of anti-polyglutamine immunohistochemistry in this study
indicate that cytoplasmic aggregation of mutant AR is
more frequent in the patients with a shorter CAG repeat.
Taken together, the differential accumulation pattern of
mutant AR between motor and sensory neurons, and their
differential correlation to CAG repeat size may be the
pathophysiological background for the development of
motor- and sensory-dominant phenotypes.

In conclusion, the results of the present study
are unequivocal electrophysiological phenotypes, motor-
dominant, sensory-dominant and non-dominant, especially
in young patients of SBMA. These features are dependent
on the CAG repeat size within the AR gene, with a longer
CAG repeat size is more closely related to the motor-
dominant phenotype and a shorter CAG repeat size related
to the sensory-dominant phenotype. Our observations shed
light on new roles of CAG repeat size in the clinical
presentation of SBMA.

Supplementary materials

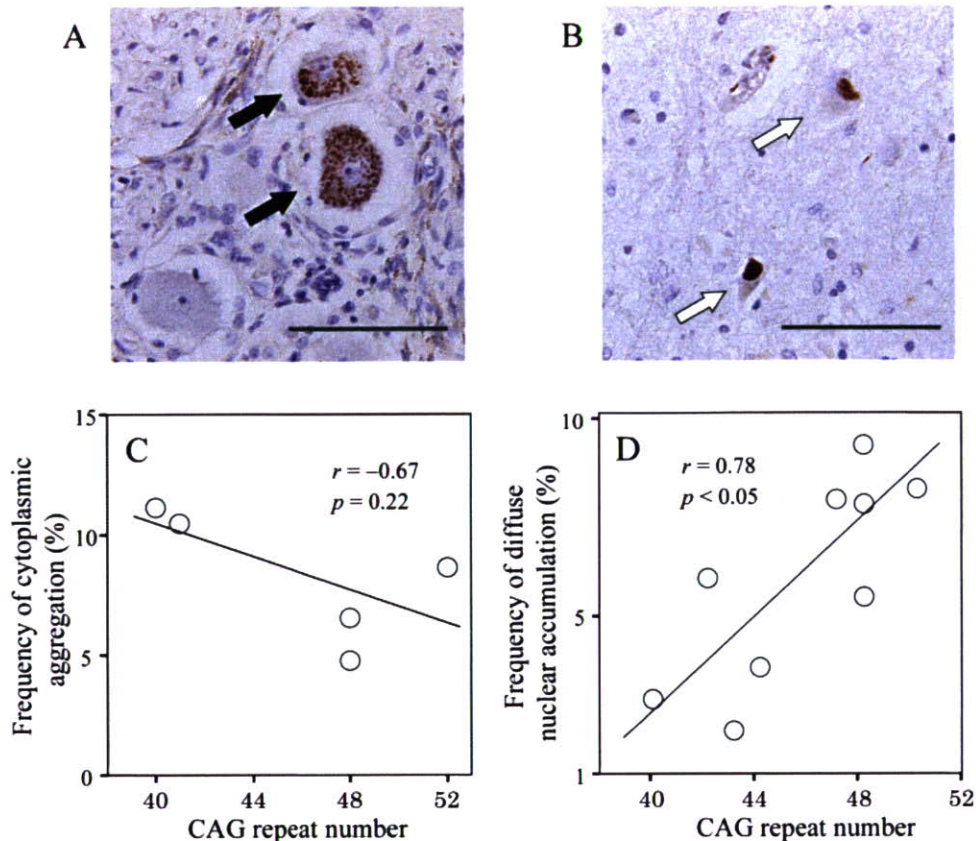Supplementary materials are available at *Brain* online.

Fig. 4 Immunohistochemical analyses of mutant androgen receptor (AR) accumulation in the dorsal root ganglion (DRG) and that in the spinal anterior horn of SBMA patients. (**A**) Aggregates of mutant AR in the cytoplasm of DRG neurons (black arrows). Scale bar = 100 μm. (**B**) Mutant AR accumulates in the motor neuron nuclei (white arrows). Scale bar = 100 μm. (**C**) Relation between the CAG repeat size and cytoplasmic aggregations in the primary sensory neuron. Cytoplasmic aggregation tended to be more frequent in the patients with a shorter CAG repeat. (**D**) Relation between the CAG repeat size and diffuse nuclear accumulation of mutant AR in the spinal motor neuron. Panel D is reconstructed from the previous report (Adachi *et al.*, 2005).

References

Adachi H, Katsuno M, Minamiyama M, Waza M, Sang C, Nakagomi Y, et al. Widespread nuclear and cytoplasmic accumulation of mutant androgen receptor in SBMA patients. Brain 2005; 128: 659–70.

Andrew SE, Goldberg YP, Hayden MR. Rethinking genotype and phenotype correlations in polyglutamine expansion disorders. Hum Mol Genet 1997; 6: 2005–10.

Antonini G, Gragnani F, Romaniello A, Pennisi EM, Morino S, Ceschin V, et al. Sensory involvement in spinal-bulbar muscular atrophy (Kennedy's disease). Muscle Nerve 2000; 23: 252–8.

Atsuta N, Watanabe H, Ito M, Banno H, Suzuki K, Katsuno M, et al. Natural history of spinal and bulbar muscular atrophy (SBMA): a study of 223 Japanese patients. Brain 2006; 129: 1446–55.

Banno H, Adachi H, Katsuno M, Suzuki K, Atsuta N, Watanabe H, et al. Mutant androgen receptor accumulation in spinal and bulbar muscular atrophy scrotal skin: a pathogenic marker. Ann Neurol 2006; 59: 520–6.

Chevalier-Larsen ES, O'Brien CJ, Wang H, Jenkins SC, Holder L, Lieberman AP, et al. Castration restores function and neurofilament alterations of aged symptomatic males in a transgenic mouse model of spinal and bulbar muscular atrophy. J Neurosci 2004; 24: 4778–86.

Doyu M, Sobue G, Mukai E, Kachi T, Yasuda T, Mitsuma T, et al. Severity of X-linked recessive bulbospinal neuronopathy correlates with size of the tandem CAG repeat in androgen receptor gene. Ann Neurol 1992; 32: 707–10.

Ferrante MA, Wilbourn AJ. The characteristic electrodiagnostic features of Kennedy's disease. Muscle Nerve 1997; 20: 323–9.

Fischbeck KH. Kennedy disease. [Review]. J Inherit Metab Dis 1997; 20: 152–8.

Gatchel JR, Zoghbi HY. Diseases of unstable repeat expansion: mechanisms and common principles. Nat Rev Genet 2005; 6: 743–55.

Guidetti D, Vescovini E, Motti L, Ghidoni E, Gemignani F, Marbini A, et al. X-linked bulbar and spinal muscular atrophy, or Kennedy disease: clinical, neurophysiological, neuropathological, neuropsychological and molecular study of a large family. J Neurol Sci 1996; 135: 140–8.

Harding AE, Thomas PK, Baraitser M, Bradbury PG, Morgan-Hughes JA, Ponsford JR. X-linked recessive bulbospinal neuronopathy: a report of ten cases. J Neurol Neurosurg Psychiatry 1982; 45: 1012–9.

Ikeuchi T, Koide R, Tanaka H, Onodera O, Igarashi S, Takahashi H, et al. Dentatorubral-pallidoluysian atrophy: clinical features are closely related to unstable expansions of trinucleotide (CAG) repeat. Ann Neurol 1995; 37: 769–75.

Johansson J, Forsgren L, Sandgren O, Brice A, Holmgren G, Holmberg M. Expanded CAG repeats in Swedish spinocerebellar ataxia type 7 (SCA7) patients: effect of CAG repeat length on the clinical manifestation. Hum Mol Genet 1998; 7: 171–6.

Kachi T, Sobue G, Sobue I. Central motor and sensory conduction in X-linked recessive bulbospinal neuronopathy. J Neurol Neurosurg Psychiatry 1992; 55: 394–7.

Katsuno M, Adachi H, Kume A, Li M, Nakagomi Y, Niwa H, et al. Testosterone reduction prevents phenotypic expression in a transgenic mouse model of spinal and bulbar muscular atrophy. Neuron 2002; 35: 843–54.

Katsuno M, Adachi H, Doyu M, Minamiyama M, Sang C, Kobayashi Y, et al. Leuprorelin rescues polyglutamine-dependent phenotypes in a transgenic mouse model of spinal and bulbar muscular atrophy. Nat Med 2003; 9: 768–73.

Katsuno M, Sang C, Adachi H, Minamiyama M, Waza M, Tanaka F, et al. Pharmacological induction of heat-shock proteins alleviates polyglutamine-mediated motor neuron disease. Proc Natl Acad Sci USA 2005; 102: 16801–6.

Katsuno M, Adachi H, Minamiyama M, Waza M, Tokui K, Banno H, et al. Pathogenesis, animal models and therapeutics in spinal and bulbar muscular atrophy (SBMA) [Review]. Exp Neurol 2006; 200: 8–18.

Kennedy WR, Alter M, Sung JH. Progressive proximal spinal and bulbar muscular atrophy of late onset. A sex-linked recessive trait. Neurology 1968; 18: 671–680.

Kimura J. Principles and valiations of nerve conduction studies. Electrodiagnosis in diseases of nerve and muscle: principles and practice. 3rd edn. New York: Oxford University Press; 2001a. p. 91–129.

Kimura J. Assessment of individual nerves. In: Kimura J, editor. Electrodiagnosis in diseases of nerve and muscle: principles and practice. 3rd edn. New York: Oxford University Press; 2001b. p. 130–77.

Kimura J. The F wave and the A wave. In: Kimura J, editor. Electrodiagnosis in diseases of nerve and muscle: principles and practice. 3rd edn. New York: Oxford University Press; 2001c. p. 439–65.

Kimura J. The F wave and the A wave. In: Kimura J, editor. Electrodiagnosis in diseases of nerve and muscle: principles and practice. 3rd edn. New York: Oxford University Press; 2001d. p. 307–38.

Koike H, Mori K, Misu K, Hattori N, Ito H, Hirayama M, et al. Painful alcoholic polyneuropathy with predominant small-fiber loss and normal thiamine status. Neurology 2001; 56: 1727–32.

Koike H, Iijima M, Sugiura M, Mori K, Hattori N, Ito H, et al. Alcoholic neuropathy is clinicopathologically distinct from thiamine-deficiency neuropathy. Ann Neurol 2003; 54: 19–29.

La Spada AR, Wilson EM, Lubahn DB, Harding AE, Fischbeck KH. Androgen receptor gene mutations in X-linked spinal and bulbar muscular atrophy. Nature 1991; 352: 77–9.

Li M, Sobue G, Doyu M, Mukai E, Hashizume Y, Mitsuma T. Primary sensory neurons in X-linked recessive bulbospinal neuropathy: histopathology and androgen receptor gene expression. Muscle Nerve 1995; 18: 301–8.

Li M, Miwa S, Kobayashi Y, Merry DE, Yamamoto M, Tanaka F, et al. Nuclear inclusions of the androgen receptor protein in spinal and bulbar muscular atrophy. Ann Neurol 1998; 44: 249–54.

Mahant N, McCusker EA, Byth K, Graham S; Huntington Study Group. Huntington's disease: clinical correlates of disability and progression. Neurology 2003; 61: 1085–92.

Minamiyama M, Katsuno M, Adachi H, Waza M, Sang C, Kobayashi Y, et al. Sodium butyrate ameliorates phenotypic expression in a transgenic mouse model of spinal and bulbar muscular atrophy. Hum Mol Genet 2004; 13: 1183–92.

Mori K, Iijima M, Koike H, Hattori N, Tanaka F, Watanabe H, et al. The wide spectrum of clinical manifestations in Sjogren's syndrome-associated neuropathy. Brain 2005; 128: 2518–34.

Norris FH, Calanchini PR, Fallat RJ, Panchari S, Jewett B. The administration of guanidine in amyotrophic lateral sclerosis. Neurology 1974; 24: 721–8.

Olney RK, Aminoff MJ, So YT. Clinical and electrodiagnostic features of X-linked recessive bulbospinal neuronopathy. Neurology 1991; 41: 823–8.

Perutz MF, Pope BJ, Owen D, Wanker EE, Scherzinger E. Aggregation of proteins with expanded glutamine and alanine repeats of the glutamine-rich and asparagine-rich domains of Sup35 and of the amyloid beta-peptide of amyloid plaques. Proc Natl Acad Sci USA 2002; 99: 5596–600.

Polo A, Teatini F, D'Anna S, Manganotti P, Salviati A, Dallapiccola B, et al. Sensory involvement in X-linked spino-bulbar muscular atrophy (Kennedy's syndrome): an electrophysiological study. J Neurol 1996; 243: 388–92.

Sakahira H, Breuer P, Hayer-Hartl MK, Hartl FU. Molecular chaperones as modulators of polyglutamine protein aggregation and toxicity. [Review]. Proc Natl Acad Sci USA 2002; 99 (Suppl 4): 16412–8.

Sobue G, Hashizume Y, Mukai E, Hirayama M, Mitsuma T, Takahashi A. X-linked recessive bulbospinal neuronopathy. A clinicopathological study. Brain 1989; 112: 209–32.

Sobue G, Doyu M, Kachi T, Yasuda T, Mukai E, Kumagai T, et al. Subclinical phenotypic expressions in heterozygous females of X-linked recessive bulbospinal neuronopathy. J Neurol Sci 1993; 117: 74–8.

Sone J, Hishikawa N, Koike H, Hattori N, Hirayama M, Nagamatsu M, et al. Neuronal intranuclear hyaline inclusion disease showing motor-sensory and autonomic neuropathy. Neurology 2005; 65: 1538–43.

Sperfeld AD, Karitzky J, Brummer D, Schreiber H, Haussler J, Ludolph AC, et al. X-linked bulbospinal neuronopathy: Kennedy disease. Arch Neurol 2002; 59: 1921–6.

Takeyama K, Ito S, Yamamoto A, Tanimoto H, Furutani T, Kanuka H, et al. Androgen-dependent neurodegeneration by polyglutamine-expanded human androgen receptor in Drosophila. Neuron 2002; 35: 855–64.

Tanaka F, Doyu M, Ito Y, Matsumoto M, Mitsuma T, Abe K, et al. Founder effect in spinal and bulbar muscular atrophy (SBMA). Hum Mol Genet 1996; 5: 1253–7.

Tanaka F, Reeves MF, Ito Y, Matsumoto M, Li M, Miwa S, et al. Tissue-specific somatic mosaicism in spinal and bulbar muscular atrophy is dependent on CAG-repeat length and androgen receptor-gene expression level. Am J Hum Genet 1999; 65: 966–73.

The ALS CNTF Treatment Study (ACTS) Phase I-II Study Group. The amyotrophic lateral sclerosis functional rating scale: Assessment of activities of daily in patients with ALS. Arch Neurol 1996; 53: 141–7.

Waza M, Adachi H, Katsuno M, Minamiyama M, Sang C, Tanaka F, et al. 17-AAG, an Hsp90 inhibitor, ameliorates polyglutamine-mediated motor neuron degeneration. Nat Med 2005; 11: 1088–95.

Zoghbi HY, Orr HT. Glutamine repeats and neurodegeneration [Review]. Annu Rev Neurosci 2000; 23: 217–47.

The Video Images of Sleep Attacks in Parkinson's Disease

Masaaki Hirayama, MD, PhD,*
Tomohiko Nakamura, MD, PhD, Norio Hori, MD,
Yasuo Koike, MD, PhD, and Gen Sobue, MD, PhD

Department of Neurology, Nagoya University Graduate
School of Medicine, Nagoya, Aichi, Japan

Video ⊂ ⊙ ⊃

Abstract: We describe a sleep attack, which was induced by taking excessive levodopa and pergolide, in a 73-year-old woman with Parkinson's disease. At the onset of the sleep attack, her head suddenly sagged and sometimes hit the table, but she did not notice these symptoms. Her family noticed that this sleep attack occurred when she began to speak slowly. Her family recorded this attack with a video camera. This sleep attack resolved with control of her medication. This is the first report of video images of a sleep attack due to excessive levodopa and a dopamine agonist. © 2007 Movement Disorder Society

- 60 -

Daytime sleep attacks have been reported in Parkinson's disease (PD) patients on a dopamine agonist or levodopa (L-dopa) treatment. However, the actual prevalence and ultimate significance of sleep attacks in PD remain controversial.[1] Some doubt has been expressed over whether the attack really does occur suddenly and without heralding symptoms in these patients, and it has been hypothesized that sleep attack may be preceded by a sleepiness of which the patients are unaware. Our knowledge of sleep attack in PD is based mainly on reports from the patients or their families. No videographic demonstration of this sleep attack has been reported. We report the clinical and videographic findings of a sleep attack in one PD patient after she took excessive L-dopa and pergolide.

CASE REPORT

A 73-year-old woman was diagnosed as having PD at age 60 when a tremor at rest and hypokinesia developed in her right upper limb. Her initial response to levodopa (carbidopa 10/levodopa 100) 200 mg/day was excellent but was complicated by response fluctuations later in the course of the disease. We increased levodopa to 400 mg/day, although the wearing-off phenomenon occurred. Therefore treatment with pergolide was started when she was 68-years old, and gradually its dose was increased to 500 μg/day. She developed mild hallucinations such as seeing a cat or children in the evening. But at the age of 70, severe wearing- off phenomenon appeared, she could not walk for about 1 hour at 10 AM and 3 PM. Pergolide was gradually increased to 1500 μg/day. However, the on-period with dyskinesia and the severe off-period continued. Accordingly, we tried treatment with cabergoline or selegiline hydrochloride, but we could not continue these drugs because of severe hallucinations. The on-period with dyskinesia sometimes appeared because she frequently took additional levodopa and pergolide without physician approval when she could not move. We tried to keep her dose of medicines appropriate to her condition, but she often took excessive levodopa and pergolide. At the age of 72, she started to have daytime sleep attacks while watching television and eating meals several times per week. At the onset of the sleep attacks, her head would suddenly sag and sometimes hit the table. On other occasions, she would drop a cup or other items that she might be holding. Although she did not notice these symptoms, her family became aware of these sleep attacks when she began to speak slowly. Her family recorded this attack using a cellular phone with a video

camera. We concluded that this episode was a sleep attack after viewing the video images, and therefore tried to better control the doses of her medications (levodopa and pergolide). Since then these sleep attacks have not recurred. We believe that these sleep attacks were a side effect of excessive doses of levodopa and pergolide. There was no indication of any prior sleep disorder in terms of the International Classification of Sleep Disorders V. In particular, no anamnestic indications of insomnia, restless legs syndrome, narcolepsy, or sleep apnea could be ascertained. Her EEG findings were normal, and there was no evidence of a sleep stage within 5 minutes or sleep onset REM (SOREM) sleep period. A brain MRI showed no abnormality for her age. SPECT with ECD showed no cerebral deficits. A polysomnographic study and multiple sleep latency test (MSLT) could not be carried out due to her lack of cooperation. HLA-typing (DR2, DQ1) was negative for narcolepsy. The Epworth sleepiness scale (ESS) was three points as scored by the patient but was 15 points on the basis of information from her family

Video Imaging

Her family noticed that she always acted peculiar before a sleep attack. Her daughter took a video of two attacks using a cellular phone with a camera. Thus, these video images are slightly grainy, but we can clearly see the nature of these sleep attacks.

Segment 1.

Her family noticed that she spoke in a sleepy tone. She tried to take a cup, but she could not. She dropped her head and fell into an approximately 30-second sleep episode with waggling of her head. She woke up suddenly. She did not remember anything of what happened.

Segment 2.

She spoke slowly, then suddenly dropped her head backward. She waggled her face and made a silent gesture with her mouth. She made a motion with her left hand on her face after a few seconds. She woke up suddenly. She did not remember anything of what happened.

DISCUSSION

This is the first report of capturing shooting a sleep attack movement on video. Unfortunately, we did not witness this attack or shoot a video in the hospital because her doses of drugs were appropriately modified. The quality of these video images from a cell phone camera was limited, but nonetheless the images had captured well the essence of the sleep attacks. Both video images showed common distinctive features. The patient

behaved in a sleep-like manner, and then lost her body tone. She slept for several tens of seconds, but continued to exhibit some automatic behaviors. She then woke up suddenly. These attacks were frequently seen after taking a meal. We concluded that these attacks were not epilepsy, because her EEG findings showed no epileptic discharge and the sleep attack disappeared after reducing the dose of levodopa and pergolide.

The report of a polysomnographic study showed that the REM latency was shorter in such patients than normal.[2] A report on MSLT documented its shorter latency. There have been some reports of a narcolepsy-like phenotype in patients with Parkinson's disease.[3-5] Her video images resembled narcolepsy clinically, although the sleep attack resolved after reducing her medication. Furthermore, no HLA-typing suggestive of narcolepsy was found.

The role of dopaminergic medications in sleep attack is not understood. Neither functional imaging of the dopamine transporter nor dopamine denervation has demonstrated any correlation between the dopamine system and sleepiness.[1] A weak but significant correlation was, however, found between the daily dose of levodopa, or a levodopa equivalent, and sedation.[1] The recently discovered neuropeptide hypocretin is important in maintaining wakefulness and its deficiency results in narcolepsy/cataplexy.[6] Some studies have found that the cerebrospinal fluid hypocretin-1 levels were normal in PD patients with daytime sleepiness,[7] but hypocretin neurotransmission is affected in PD.[8] 1-methyl-4-phenyl-1,2,3,6-tetrahydropyridine1-methyl-4-phenyl-1,2,3,6-tetrahydropyridine-treated mice have increased amounts of REM sleep.[9] Hyperdopamine exposure induced electrophysiological REM activity in the hippocampal area of mice.[10] Furthermore, a D2 dopamine receptor agonist restored this REM activity.[10] Taken together, these data suggest that this sleep attack phenomenon could be a hypersensitivity or a hyperdose reaction to the D2 receptor.

In these patients with sleep attack, the ESS has been reported to be normal.[11,12] In addition, this patient did not notice her sleep attack and sleepiness. Thus, information from a patient's family is very important for diagnosing a

REFERENCES

1. Arnulf I. Excessive daytime sleepiness in parkinsonism. Sleep Med Rev 2005;9:185-200.
2. Ulivelli M, Rossi S, Lombardi C, et al. Polysomnographic characterization of pergolide-induced sleep attacks in idiopathic PD. Neurology 2002;58:462-465.
3. Arnulf I, Bonnet AM, Damier P, et al. Hallucinations, REM sleep, and Parkinson's disease: a medical hypothesis. Neurology 2000; 55:281-288.
4. Moller JC, Stiasny K, Hargutt V, et al. Evaluation of sleep and driving performance in six patients with Parkinson's disease re-

porting sudden onset of sleep under dopaminergic medication: a pilot study. Mov Disord 2002;17:474-481.
5. Rye DB, Bliwise DL, Dihenia B, Gurecki P. FAST TRACK: daytime sleepiness in Parkinson's disease. J Sleep Res 2000;9:63-69.
6. Overeem S, Mignot E, van Dijk JG, Lammers GJ. Narcolepsy: clinical features, new pathophysiologic insights, and future perspectives. J Clin Neurophysiol 2001;18:78-105.
7. Overeem S, van Hilten JJ, Ripley B, Mignot E, Nishino S, Lammers GJ. Normal hypocretin-1 levels in Parkinson's disease patients with excessive daytime sleepiness. Neurology 2002;58:498-499.
8. Fronczek R, Overeem S, Lee SY, et al. Hypocretin (orexin) loss in Parkinson's disease. Brain 2007;130 (Part 6):1577-1585.
9. Monaca C, Laloux C, Jacquesson JM, et al. Vigilance states in a parkinsonian model, the MPTP mouse. Eur J Neurosci 2004;20: 2474-2478.
10. Dzirasa K, Ribeiro S, Costa R, et al. Dopaminergic control of sleep–wake states. J Neurosci 2006;26:10577-10589.
11. Korner Y, Meindorfner C, Moller JC, et al. Predictors of sudden onset of sleep in Parkinson's disease. Mov Disord 2004;19:1298-1305.
12. Tan EK, Lum SY, Fook-Chong SM, et al. Evaluation of somnolence in Parkinson's disease: comparison with age- and sex-matched controls. Neurology 2002;58:465-468.

Original Article

Widespread spinal cord involvement in progressive supranuclear palsy

Yasushi Iwasaki,[1] **Mari Yoshida,**[2] **Yoshio Hashizume,**[2] **Manabu Hattori,**[3] **Ikuko Aiba**[4] **and Gen Sobue**[1]

[1]Department of Neurology, Nagoya University Graduate School of Medicine, Nagoya, [2]Department of Neuropathology, Institute for Medical Science of Aging, Aichi Medical University, Aichi-gun, [3]Department of Neurology and Neuroscience, Nagoya City University Graduate School of Medical Science, Nagoya, and [4]Department of Neurology, National Hospital Organization Higashi Nagoya National Hospital, Nagoya, Japan

We describe the histopathologic features of spinal cord lesions in 10 cases of progressive supranuclear palsy (PSP) and review the literature. Histologic examination revealed atrophy with myelin pallor in the anterior funiculus and anterolateral funiculus in the cervical and thoracic segments in eight of the 10 cases, whereas the posterior funiculus was well preserved. The degrees of atrophy of the anterior funiculus and the anterolateral funiculus correlated with that of the tegmentum of the medulla oblongata. Myelin pallor of the lateral corticospinal tract was observed in two of the 10 cases. Microscopic observation of the spinal white matter, particularly the cervical segment, revealed a few to several neuropil threads, particularly in the white matter surrounding the anterior horn after Gallyas-Braak (GB) staining or AT-8 tau immunostaining. However, the posterior funiculus was completely preserved from the presence of argyrophilic or tau-positive structures. In the spinal gray matter, widespread distribution of neurons with cytoplasmic inclusions and neuropil threads was observed, particularly in the medial division of the anterior horn and intermediate gray matter, especially in the cervical segment. Globose-type neurofibrillary tangles and pretangles were found. The distribution of GB- or AT-8 tau-positive small neurons and neuropil threads resembled that of the spinal interneurons. In conclusion, the spinal cord, especially the cervical segment, is constantly involved in the pathologic process of PSP. We speculate that spinal interneurons and their neuronal processes, particularly in the medial division of the anterior horn and intermediate gray matter of the cervical segment, are most severely damaged in the PSP spinal cord.

Key words: neuronal inclusion, neuropil threads, progressive supranuclear palsy, spinal cord lesion, tract degeneration.

INTRODUCTION

Progressive supranuclear palsy (PSP) was first described and defined as a clinicopathologic entity by Steele *et al.* in 1964.[1] The neuropathologic features of PSP are neuronal loss and astrocytosis with neurofibrillary tangles (NFTs), which are observed mainly in the basal ganglia, brainstem and cerebellum.[1–3] In addition, abnormal glial cytoskeletal structures such as glial fibrillary tangles (GFTs), including tuft-shaped astrocytes and coiled bodies and neuropil threads, are found around these lesions.[2–5] PSP is considered a discrete clinicopathologic entity;[3–6] however, the pathophysiologic mechanisms underlying the lesions are not completely understood. Although spinal cord abnormalities are generally considered uncommon in cases of PSP,[2] there have been some reports of spinal cord lesions in patients with PSP, and the morphologic changes have been described.[1,7–15] Three notable studies were recently reported,[16–18] and the spinal cord is now considered to be one of the regions involved in PSP. In the present study, we systematically examined the spinal cords in 10 cases of PSP using the Gallyas-Braak (GB) impregnation technique[4,5] and AT-8 tau immunostaining,[19] paying particular attention to the tract degeneration and neuronal and glial tau pathology.

MATERIALS AND METHODS

Ten autopsy cases of PSP from the Institute for Medical Science of Aging, Aichi Medical University, were included

Table 1 Clinical summary of 10 cases of progressive supranuclear palsy

Patient	Sex	Age at onset (years)	Age at death (years)	Disease duration (years)	Brain weight (g)	Clinical symptoms and signs				
						Initial symptom	Gaze palsy	Axial rigidity	Nuchal dystonia	Other neurologic signs
1	F	74	75	2	1120	Gait disturbance	+	+	+	Dementia, frequent falls
2	F	58	62	4	1090	Gait disturbance	+	+	+	Akinesia, dementia, frequent falls
3	F	79	84	4	1090	Gait disturbance	+	+	+	Dementia, frequent falls
4	M	76	81	6	1150	Gait disturbance	+	+	+	Dementia, frequent falls
5	F	66	72	6	1080	Tremor of legs	+	+	+	Dementia, hallucination, Frequent falls
6	M	68	75	7	1120	Dysarthria	+	+	+	Frequent falls
7	M	61	68	7	1060	Gait disturbance	+	+	+	Dementia
8	M	71	78	7	1150	Micrographia	+	+	+	Frequent falls
9	F	60	69	9	980	Gait disturbance	+	+	+	Frequent falls
10	M	67	78	11	1120	Gait disturbance	+	+	+	Tremor, frequent falls

in the present study. All patients had typical clinicopathologic features of PSP in accordance with the National Institute of Neurological Disorders (NINDS) and Society of Progressive Supranuclear Palsy (SPSP) and preliminary NINDS diagnostic criteria.[6,20] Tuft-shaped astrocytes, a disease-specific hallmark of PSP,[4,5] were also identified in the cerebral neocortex and the basal ganglia in all patients. For control, spinal cords were collected from eight autopsied patients judged by neuropathologic examination to be free from neurologic degeneration and who did not have neurologic signs or symptoms. The PSP patients comprised five men and five women (mean age at death, 74.2 ± 6.6 years; range, 62–84 years), and control subjects comprised three men and five women (mean age at death, 70.6 ± 5.1 years; range, 61–76 years). Mean disease duration in the PSP patients was 6.3 ± 2.6 years (range, 2–11 years). Clinical data for the PSP patients, arranged in order of disease duration, are summarized in Table 1.

The entire spinal cord of each patient was fixed in neutral formalin for several weeks. Segmental blocks including cervical, thoracic and lumbosacral segments were embedded in paraffin, and 8-μm-thick horizontal sections were then prepared. For routine neuropathologic examination, sections were processed with hematoxylin and eosin (H&E), Klüver-Barrera (KB), Holzer, Bodian silver and GB stains. Immunohistochemistry was carried out with antibodies against phosphorylation-dependent tau (AT-8, mouse monoclonal, diluted 1:3000; Innogenetics, Ghent, Belgium) and glial fibrillary acidic protein (GFAP, mouse monoclonal, diluted 1:400; DAKO, Glostrup, Denmark). Antibody binding was detected by a labeled streptavidin-biotin (LSAB) method with a DAKO LSAB kit (DAKO). The immunostaining protocol was as described previously.[19]

We assessed atrophy, myelin pallor, gliosis, neuronal loss and the presence of NFTs, GFTs and neuropil threads semiquantitatively. Spinal cord atrophy and myelin pallor

were assessed in KB-stained samples. Neuronal loss was assessed in the HE- or KB-stained samples. Neurons in the spinal gray matter were classified as large (approximately >33 μm), medium (approximately > 25 – < 33 μm) or small (approximately < 25 μm), according to results of a previous study.[21] The presence of gliosis was judged from the sections treated with the H&E and Holzer stains and GFAP immunostaining. Typical NFTs were identified by Bodian silver staining. We identified neuronal inclusions, GFTs such as tuft-shaped astrocytes and coiled bodies, and neuropil threads in GB-stained and AT-8-tau immunostained sections. Microscopic fields for at least six different levels of the cervical segment, 12 levels of the thoracic segment and six levels of the lumbosacral segment were observed. Furthermore, we looked for correlation between the medulla oblongata and the spinal cord by observing the changes in many sections. The white matter and gray matter of the spinal cord were subdivided into several regions as shown in Tables 2–5, and respective lesions were assessed by semiquantitative analysis. Atrophy of the medulla oblongata and spinal cord atrophy and myelin pallor were assessed as severe (+++), moderate (++), mild (+), very mild (+/–) or none (–). Neuropil threads in the white and gray matter were evaluated by density as numerous (+++), moderate (++), several (+), a few (+/–) or none (–) in the respective regions. Neurons with cytoplasmic inclusions in the gray matter were counted in the respective regions at each spinal segment and averaged as more than six positive neurons (+++), 3–6 positive neurons (++), 1–3 positive neurons (+), 0–1 positive neurons (+/–) or no positive neurons (–). Spearman's rank correlation coefficient was calculated to assess the relation between pathologic features and between pathologic features and clinical measures. Statistical analysis was performed with Excel 2000 (Microsoft, Redmond, WA, USA) and the add-in software Statcel 2 (OMS, Tokyo, Japan).

Table 2 Histologic features shown by Kluver-Barrera staining in the spinal white matter of progressive supranuclear palsy patients

+++, severe; ++, moderate; +, mild; ±, very mild; −, none. AF, anterior funiculus includes the anterior corticospinal tract and medial longitudinal fasciculus; ALF, anterolateral funiculus; LCT, lateral corticospinal tract; PF, posterior funiculus.

RESULTS

Histologic findings

In eight of the 10 cases, the anterior funiculus and anterolateral funiculus of the cervical and thoracic segments in the KB-stained sections showed atrophy and myelin pallor (Table 2, Fig. 1). In the anterior funiculus and anterolateral funiculus of the cervical white matter, the degree of atrophy correlated with the degree of myelin pallor (in the anterior funiculus, $r_s = 0.98$ and $P < 0.01$; in the anterolateral funiculus, $r_s = 0.98$ and $P < 0.01$). The macroscopic appearances of the posterior funiculus and gray matter were unremarkable.

Tract degeneration

The degrees of atrophy of the anterior funiculus and the anterolateral funiculus in the cervical white matter correlated with that of the tegmentum of the medulla oblongata (between the tegmentum and the anterior funiculus, $r_s = 0.91$ and $P < 0.01$; between the tegmentum and the anterolateral funiculus, $r_s = 0.98$ and $P < 0.01$). Myelin pallor of the lateral corticospinal tract was seen in two of the 10 cases (Table 2, Fig. 1).

Neuronal loss and gliosis

Mild gliosis was revealed by H&E staining, Holzer staining and GFAP immunostaining in the cervical gray matter, particularly in the medial division of the anterior horn and intermediate gray matter. Although the number of small neurons in the medial division of the anterior horn and intermediate gray matter in the cervical segment appeared moderately decreased in cases of PSP, the number of large motor neurons in the anterior horn was relatively normal. The numbers of neurons in the intermediolateral column, Clarke's column and posterior horn were also normal. The number of neurons of Onufrowicz nucleus was moderately decreased.

Tau pathology

White matter

In the white matter of the PSP spinal cords, a few to several neuropil threads and a few coiled bodies were observed in the anterior funiculus and anterolateral funiculus in all cases (Fig. 2), whereas tuft-shaped astrocytes were not seen in the white matter by GB staining or AT-8 tau immunostaining. Detection of neuropil threads in the spinal white matter by GB staining is summarized in Table 3. Although the density of neuropil threads varied from case to case, these structures were observed most frequently in the white matter surrounding the anterior horn, especially in

Table 3   Number of neuropil threads detected by Gallyas-Braak staining in the spinal white matter of progressive supranuclear palsy patients

Patient	Cervical segment				Thoracic segment				Lumbosacral segment			
	AF	ALF	LCT	PF	AF	ALF	LCT	PF	AF	ALF	LCT	PF
1	±	–	–	–	–	–	–	–	–	–	–	–
2	+	+	–	–	±	–	–	–	–	–	–	–
3	+	±	–	–	±	–	–	–	±	–	–	–
4	+	±	–	–	±	–	–	–	–	–	–	–
5	±	±	–	–	–	–	–	–	–	–	–	–
6	±	±	–	–	±	–	–	–	–	–	–	–
7	±	±	–	–	–	–	–	–	–	–	–	–
8	±	–	–	–	–	–	–	–	–	–	–	–
9	±	–	–	–	±	–	–	–	–	–	–	–
10	±	–	–	–	–	–	–	–	–	–	–	–

+++, numerous; ++, moderate; +, several; ±, a few; –, none. AF, anterior funiculus includes the anterior corticospinal tract and medial longitudinal fasciculus; ALF, anterolateral funiculus; LCT, lateral corticospinal tract; PF, posterior funiculus.

Table 4   Neurons with cytoplasmic inclusions detected by Gallyas-Braak staining in the spinal gray matter of progressive supranuclear palsy patients

Patient	Cervical segment				Thoracic segment			Lumbosacral segment			
	AH		IGM	PH	AH	IGM	PH	AH		IGM	PH
	MD	LD						MD	LD		
1	±	±	+	±	±	+	±	–	–	+	–
2	±	±	+	+	–	–	–	–	–	±	–
3	+	+	+++	+	±	+	±	±	±	+	±
4	+	+	++	+	+	+	+	±	±	±	±
5	±	±	+	±	±	+	±	–	–	±	–
6	+	+	++	+	±	+	±	±	–	±	–
7	±	±	++	+	±	+	±	±	±	+	+
8	+	+	+++	+	±	+	±	±	±	+	±
9	+	+	++	+	±	+	±	±	–	+	±
10	+	+	++	±	±	+	±	±	±	±	±

+++, more than 6 positive neurons; ++, 3-6 positive neurons; +, 1-3 positive neurons; ±, 0-1 positive neurons; –, no positive neuron. AH, anterior horn; IGM, intermediate gray matter; LD, lateral division; MD, medial division; PH, posterior horn.

Table 5   Number of neuropil threads detected by Gallyas-Braak staining in the spinal gray matter of progressive supranuclear palsy patients

Patient	Cervical segment				Thoracic segment			Lumbosacral segment			
	AH		IGM	PH	AH	IGM	PH	AH		IGM	PH
	MD	LD						MD	LD		
1	++	+	+++	±	++	++	±	–	–	±	–
2	+++	++	++	+	±	±	±	–	–	±	–
3	+++	++	+++	+	++	++	+	+	+	++	+
4	+++	++	+++	+	++	++	+	+	+	+	+
5	++	+	++	+	+	+	±	+	+	+	±
6	++	+	++	+	+	++	±	+	±	+	–
7	++	+	++	+	++	++	±	+	+	+	±
8	++	++	++	+	+	+	±	±	±	+	+
9	++	++	+++	+	+	++	+	+	±	+	±
10	+	+	++	±	+	+	±	±	±	+	±

+++, numerous; ++, moderate; +, several; ±, a few; –, none. AH, anterior horn; IGM, intermediate gray matter; LD, lateral division; MD, medial division; PH, posterior horn.

the medial longitudinal fasciculus and the reticular formation of the anterior funiculus. These findings were more conspicuous in the cervical segment than in the thoracolumbosacral segment. In the anterior funiculus and ante-rolateral funiculus of the cervical white matter, the degree of atrophy did not correlate with the number of neuropil threads (in the anterior funiculus, $r_s = -0.28$ and $P = 0.40$; in the anterolateral funiculus, $r_s = -0.36$ and $P = 0.28$). The

posterior funiculus was completely preserved from the presence of GB- or AT-8 tau-positive structures.

Gray matter

Gallyas-Braak staining and AT-8 tau immunostaining revealed argyrophilic and tau-positive structures including GFTs such as tuft-shaped astrocytes and coiled bodies, numerous neuropil threads and neuronal inclusions in the spinal gray matter (Fig. 3). Detection of neurons with cytoplasmic inclusions and neuropil threads in the spinal gray matter by GB staining is summarized in Tables 4 and 5, respectively. Many argyrophilic or tau-positive neuronal inclusions were observed, particularly in the small neurons in the intermediate gray matter, and such inclusions were relatively sparse in the lateral division of the anterior horn and posterior horn (Fig. 4). These positively stained neurons were observed more frequently in the cervical segment than in the thoracolumbosacral segment. Neither age at onset nor disease duration correlated with the number of neurons with cytoplasmic inclusions in the cervical intermediate gray matter (between age at onset and the number of positive neurons, $r_s = 0.50$ and $P = 0.13$; between the disease duration and the number of positive neurons, $r_s = 0.44$ and $P = 0.18$). Neuronal inclusions were of the globose type, suggestive of NFTs (Fig. 3a), or showed diffuse granular accumulation of cytoplasmic tau, suggestive of pretangles (Fig. 3b). A few neuronal inclusions were seen in the large motor neurons of the anterior horn, intermediolateral column and Clarke's column, and some large motor neurons showed filamentous cytoplasmic inclusions (Fig. 3c). In contrast to the GB-stained and AT-8-immunostained sections, the Bodian silver-stained sections showed a few typical NFTs. The typical NFTs revealed by Bodian silver staining were of the globose type (Fig. 3d) and located mainly in the intermediate gray matter and the basal portion of the posterior horn, but they were not observed in large motor neurons in the anterior horn.

The number of neuropil threads was much greater in the gray matter than in the white matter. The density of neuropil threads varied between patients, but the distribution pattern was relatively uniform and prominent in the medial division of anterior horn and intermediate gray matter (Fig. 5). These conditions were observed more frequently in the cervical segment than in the thoracolumbosacral segment. In the anterior horn of the cervical segment, neuropil threads were prominent in the medial division, and they decreased in density toward the lateral division. In the intermediate gray matter, neuropil threads were prominent in the lateral portion, and they decreased in density toward the medial portion. In the posterior horn, neuropil threads were observed most frequently in the basal portion, and a few were seen in the substantia gelatinosa and the substan-
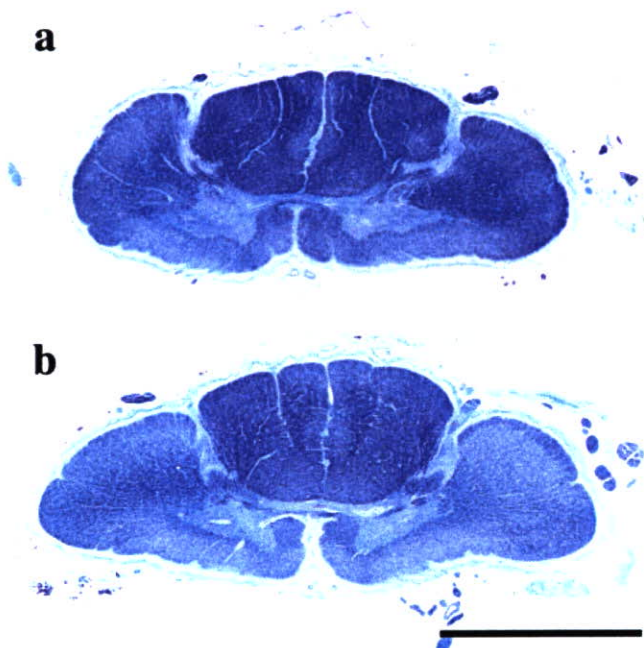

Fig. 1 Representative images of the cervical segments from two patients with progressive supranuclear palsy (PSP). The anterior and anterolateral funiculus showed atrophy and myelin pallor. These two cases also showed myelin pallor of the lateral corticospinal tract (a: patient 8, b: patient 9, Klüver-Barrera staining). Bar = 5 mm.
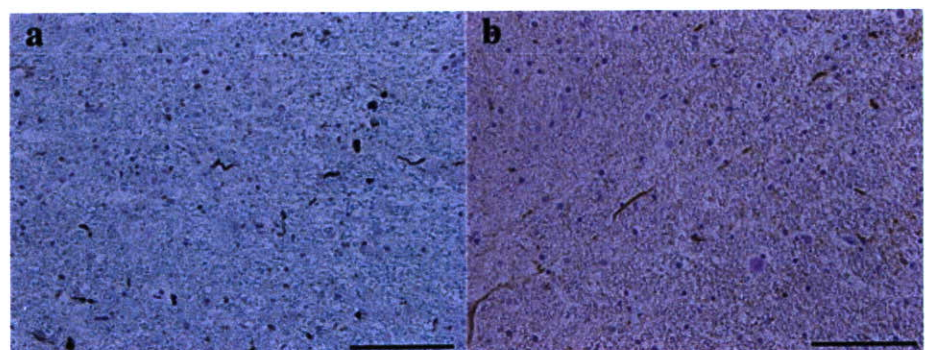

Fig. 2 White matter lesions of the progressive supranuclear palsy (PSP) spinal cord. Several neuropil threads are present in the white matter surrounding the anterior horn (a: patient 4, Gallyas-Braak staining; b: patient 7, AT-8 tau immunostaining). Bars = 100 μm.
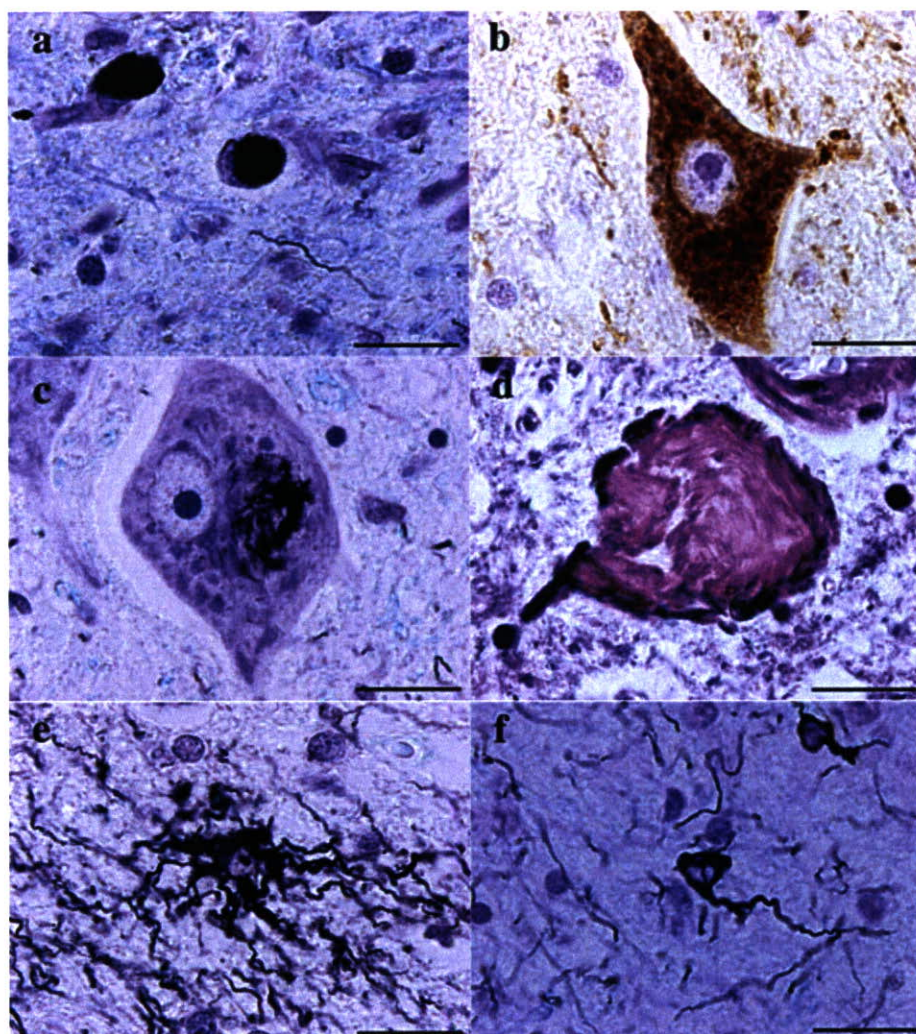
© 2007 Japanese Society of Neuropathology

Fig. 3 Representative neuronal inclusions and glial inclusions in the progressive supranuclear palsy (PSP) spinal cord. (a) Globose-type, neurofibrillary tangle (NFT)-like neuronal inclusions in intermediate gray matter in the cervical segment (patient 8, Gallyas-Braak [GB] staining). (b) Pretangle-like neuronal inclusion in a large motor neuron in the anterior horn of the cervical segment (patient 3, AT-8 tau immunostaining). (c) Filamentous cytoplasmic inclusions in a large motor neuron in the anterior horn of the cervical segment (patient 8, GB staining). (d) Typical NFT seen in the basal portion of the posterior horn (patient 3, Bodian silver staining). (e) Tuft-shaped astrocyte in the medial division of the anterior horn in the cervical segment (patient 3, GB staining). (f) Coiled body in the intermediate gray matter in the cervical segment (patient 3, GB staining). Bars = 20 µm.

tia spongiosa. Neither age at onset nor disease duration correlated with the density of neuropil threads in the cervical intermediate gray matter (between age at onset and the density of neuropil threads, $r_s = 0.56$ and $P = 0.09$; between the disease duration and the density of neuropil threads, $r_s = -0.15$ and $P = 0.66$). The density of neuropil threads did not correlate with the number of neurons with cytoplasmic inclusions in the cervical intermediate gray matter (in the medial division of the anterior horn, $r_s = 0.22$ and $P = 0.50$; in the intermediate gray matter, $r_s = 0.30$ and $P = 0.36$). The distribution of small neurons with cytoplasmic inclusions and neuropil threads was similar to that of spinal interneurons and their processes, particularly in the cervical segment.

A few tuft-shaped astrocytes were seen in the spinal gray matter (Fig. 3e), but the distribution could not be assessed because there were so few. A few to several coiled bodies were seen in the spinal gray matter (Fig. 3f); the distribution pattern was almost the same as that of neuropil threads, but they were fewer in number than the neuropil threads.

The number of AT-8 tau-positive structures was much greater than the number of GB-positive argyrophilic structures. No tau-positive or argyrophilic structures were identified in any control spinal cord.

DISCUSSION

In the original PSP report by Steele *et al.*[1] the presence of NFTs in the two examined spinal cords was briefly described. Loss of neurons in the anterior horn[7-10,12,13] and the presence of NFTs in the spinal cord have been described.[1,7,11,14] Kato *et al.* performed ultrastructural electron microscopy studies of NFTs in PSP spinal cords and reported that the NFTs consisted of bundles of straight fibrils with a diameter of approximately 15 nm[22] These NFTs were arranged in bundles of compact parallel arrays and were found to be essentially identical to the NFTs in the brain.[22] The presence of neuropil threads in the spinal white matter was described only by Umahara *et al.*[15] Recently, three notable studies pertaining to PSP spinal cord lesions were reported.[16-18] Kikuchi *et al.* showed

© 2007 Japanese Society of Neuropathology

Fig. 4 Identification of neurons with cytoplasmic inclusions in two representative progressive supranuclear palsy (PSP) cases. Many argyrophilic or tau-positive neurons were observed, particularly among the small neurons in the medial division of the anterior horn and intermediate gray matter, and such neurons were relatively sparse in the posterior horn and lateral division of the anterior horn. (a: patient 8, b: patient 3; a1: Gallyas-Braak staining, b1: AT-8 tau immunostaining, a2 and b2 show the schema of a1 and b1, respectively. Asterisks indicate positively stained neurons; cervical segment). (*AH*, anterior hor; *IMG*, intermediate gray matter; *PH*, posterior horn).
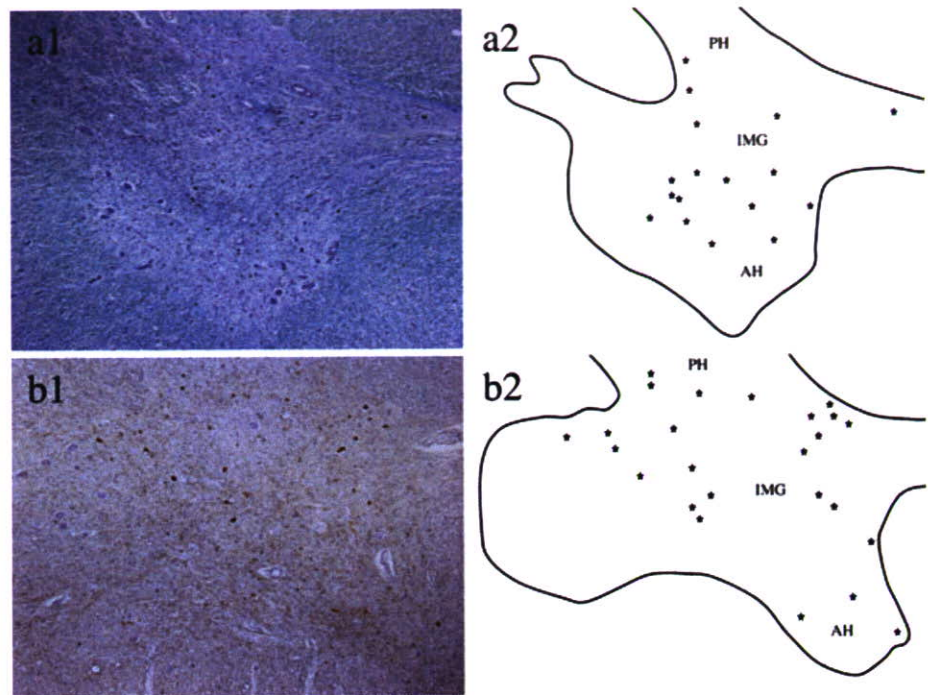
by immunohistochemistry that microtubule-associated protein-2 expression in the cervical segment was significantly decreased in the medial division of the anterior horn, intermediate gray matter and posterior horn but that there was no significant change in the substantia gelatinosa or lateral division of the anterior horn.[16] Scaravilli *et al.* investigated the Onufrowicz nucleus in three cases of PSP and found neuronal loss and the presence of NFTs, glial inclusions and neuropil threads.[17] Vitaliani *et al.* reported severe neuronal loss throughout the spinal cord in five cases of PSP.[18]

Brainstem lesions have been regarded as the primary PSP lesions.[1] Murakami *et al.* confirmed correlation between tract degeneration of the tegmentum of the medulla oblongata and that of the anterolateral funiculus of the cervical segment of the PSP spinal cord.[23] Similar tract degeneration was observed in the present study, and atrophy and myelin pallor of the anterior funiculus and anterolateral funiculus were also observed. Two of the 10 cases showed myelin pallor of the lateral corticospinal tract, indicating pyramidal tract degeneration in PSP. Interestingly, although the degree of atrophy correlated with the degree of myelin pallor, the degrees of atrophy and myelin pallor did not correlate with the number of neuropil threads in the cervical white matter. We think this discrepancy is due to the fact that tract degeneration seen in PSP-affected spinal white matter is secondary degeneration due to the tegmental involvement of the brainstem, particularly in the medulla oblongata. Furthermore, although a few to several neuropil threads were observed

mainly in the anterior funiculus and anterolateral funiculus in the PSP-affected spinal white matter, argyrophilic- or tau-positive structures were completely absent in the posterior funiculus. We speculate that this discrepancy may reflect centrifugal spread of tau pathology along the descending fibers or regional susceptibility for tau accumulation in the PSP spinal cord.

The most important finding of the present study was the identification of widespread neurons with cytoplasmic inclusions and neuropil threads in the PSP spinal cord, particularly in the cervical gray matter. Subdivision of the spinal gray matter according to Rexed's schema allowed us to determine that neurons with cytoplasmic inclusions and neuropil threads were abundant in the Rexed VI, VII and VIII layers.[24] Spinal gray matter lesions did not necessarily coexist with prominent spinal white matter lesions. The number of neurons with cytoplasmic inclusions and the density of neuropil threads did not correlate with age at onset or with disease duration. These neurons, positive for GB staining or AT-8 tau immunostaining, were mostly small neurons in the medial division of the anterior horn and intermediate gray matter and could not be easily detected by Bodian silver staining. Therefore, we speculate that most neurons with cytoplasmic inclusions, which were positive for GB staining and AT-8 tau immunostaining, were immature pretangles.[19,25] Although the density of neuropil threads and the number of neurons with cytoplasmic inclusions in the spinal gray matter varied from case to case, these features were common to all cases of PSP. Because no tau-positive structures or argyrophilic struc-
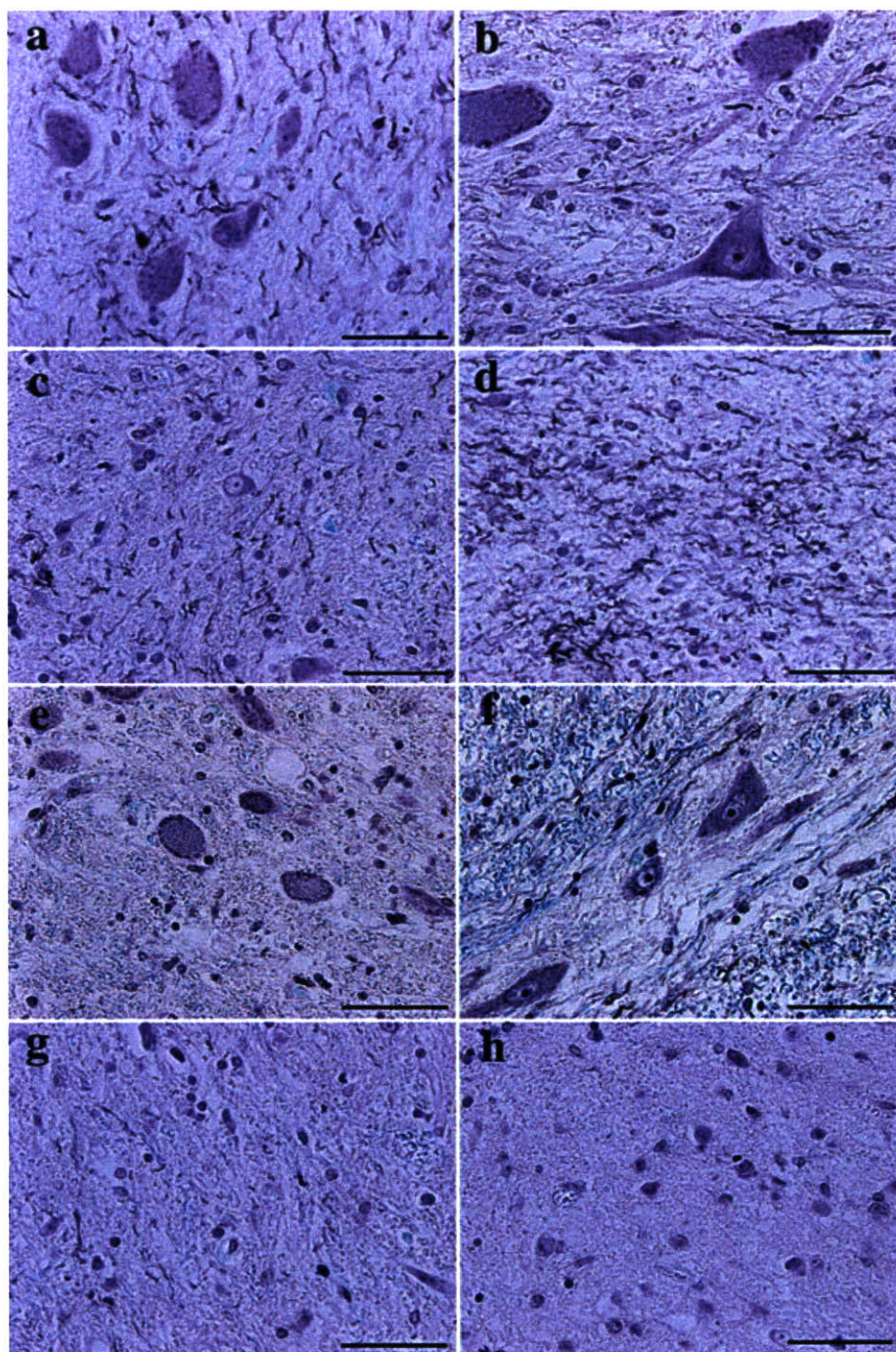
Fig. 5 Presence of neuropil threads in the gray matter lesions. (a) Medial division of the anterior horn in the cervical segment. (b) Lateral division of the anterior horn in the cervical segment. (c) Medial portion of the intermediate gray matter in the cervical segment. (d) Lateral portion of the intermediate gray matter in the cervical segment. (e) Intermediolateral column in the upper thoracic segment. (f) Clarke's column in the upper thoracic segment. (g) Basal portion of the posterior horn in the cervical segment. (h) Substantia gelatinosa of the posterior horn in the cervical segment (patient 3, Gallyas-Braak staining). Bars = 50 μm.

tures were identified in the eight control spinal cords, our results indicate that the PSP spinal cord is affected by an abnormal tau-degenerative alteration. Some authors have argued that tuft-shaped astrocytes are characteristic of PSP,[4-6,20] but only a few tuft-shaped astrocytes were seen in some PSP spinal cords in the present study.

The relation between the pathologic features of spinal cord lesions and clinical signs of PSP is not well understood. In the anterior horn of the cervical segment, passing from the most medial part to its lateral periphery, motor neurons successively innervate muscles of the trunk, shoulder, upper arm, forearm and fingers.[26] The small neurons, which are distributed in the intermediate gray matter of the spinal cord, comprise mainly interneurons.[26,27] It is noteworthy that the distribution of small neurons with cytoplasmic inclusions and neuropil threads was well matched with that of spinal interneurons and their neuronal processes in the cervical segment. The descending fibers of the extrapyramidal system, such as those of the rubrospinal tract, tectospinal tract, reticulospinal tract and

© 2007 Japanese Society of Neuropathology

medial longitudinal fasciculus, synapse with interneurons that connect to motor neurons of the anterior horn[26,27] and the spinal interneurons that mediate between input and output elements and produce varied reflex behaviors.[28] Therefore, we also speculate that these spinal gray matter lesions, particularly in the medial division of the anterior horn and intermediate gray matter of the cervical segment, cause the nuchal dystonia, retrocollis and axial rigidity characteristic of PSP patients. Similar speculation was made by Kikuchi *et al.*[16] but Vitaliani *et al.* concluded that this hypothesis could not be supported by their data.[18] Further neuropathologic investigation is needed to elucidate the underlying relations between spinal cord lesions and clinical signs of PSP.

Important findings in the present study include atrophy and myelin pallor of the anterior funiculus and anterolateral funiculus and the existence of white matter and gray matter lesions including the presence of GB- and AT-8 tau-positive cytoskeletal structures, particularly in the cervical segment. Widespread spinal cord involvement as seen in the present study suggests the presence of tract degeneration and damage of the spinal interneurons and their neuronal processes. We emphasize that these spinal cord lesions, especially in the cervical segment, should be included in the list of pathologic lesions of PSP.

REFERENCES

1. Steele JC, Richardson JC, Olszewski J. Progressive supranuclear palsy: a heterogeneous degeneration involving the brain stem, basal ganglia and cerebellum with vertical gaze and pseudobulbar palsy, nuchal dystonia and dementia. *Arch Neurol* 1964; **10**: 333–359.
2. Lowe JS, Leigh N. Disorder of movement and system degenerations. In: Graham DI, Lantos PL, eds. *Greenfield's Neuropathology*, 7th edn. London: Arnold, 2002; 337–342.
3. Duvoison RC. Progressive supranuclear palsy. In: Rowland LP, ed. *Merritt's Textbook of Neurology*, 9th edn. Baltimore, MD: Williams & Wilkins, 1995; 730–733.
4. Iwasaki Y, Yoshida M, Hattori M *et al.* Distribution of tuft-shaped astrocytes in the cerebral cortex in progressive supranuclear palsy. *Acta Neuropathol (Berl)* 2004; **108**: 399–405.
5. Hattori M, Hashizume Y, Yoshida M *et al.* Distribution of astrocytic plaques in the corticobasal degeneration brain and comparison with tuft-shaped astrocytes in the progressive supranuclear palsy brain. *Acta Neuropathol (Berl)* 2003; **106**: 143–149.
6. Hauw JJ, Daniel SE, Dickson D *et al.* Preliminary NINDS neuropathologic criteria for Steel-

7. Behrman S, Carroll JD, Janota I, Matthews WB. Progressive supranuclear palsy: clinicopathological study of four cases. *Brain* 1969; **92**: 663–678.
8. Blumenthal H, Miller C. Motor nuclear involvement in progressive supranuclear palsy. *Arch Neurol* 1969; **20**: 362–367.
9. Bugiani O, Mancardi GL, Brusa A, Ederli A. The fine structure of subcortical neurofibrillary tangles in progressive supranuclear palsy. *Acta Neuropathol (Berl)* 1979; **45**: 147–152.
10. Ishino H, Higashi H, Kuroda S, Yabuki S, Hayahara T, Otsuki S. Motor nuclear involvement in progressive supranuclear palsy. *J Neurol Sci* 1974; **22**: 235–244.
11. Kato T, Hirano A, Weinberg MN, Jacobs AK. Spinal cord lesion in progressive supranuclear palsy: some new observations. *Acta Neuropathol (Berl)* 1986; **71**: 11–14.
12. Kurihara T, Landau WM, Torack RM. Progressive supranuclear palsy with action myoclonus, seizure. *Neurology* 1974; **24**: 219–223.
13. Powell HC, London GW, Lampert PW. Neurofibrillary tangles in progressive supranuclear palsy: electron microscopic observations. *J Neuropathol Exp Neurol* 1974; **33**: 98–106.
14. Tomonaga M. Ultrastructure of neurofibrillary tangles in progressive supranuclear palsy. *Acta Neuropathol (Berl)* 1977; **37**: 177–181.
15. Umahara T, Hirano A, Kato S, Shibata N, Yen SC. Demonstration of neuropil thread-like structures in the spinal cord white matter in progressive supranuclear palsy: an immunohistochemical investigation. *Neuropathology* 1995; **15**: 103–107.
16. Kikuchi H, Doh-ura K, Kira J, Iwai T. Preferential neurodegeneration in the cervical spinal cord of progressive supranuclear palsy. *Acta Neuropathol (Berl)* 1999; **97**: 577–584.
17. Scaravilli T, Pramstaller PP, Salerno A *et al.* Neuronal loss in Onuf's nucleus in three patients with progressive supranuclear palsy. *Ann Neurol* 2000; **48**: 97–101.
18. Vitaliani R, Scaravilli T, Egarter-Vigl E *et al.* The pathology of the spinal cord in progressive supranuclear palsy. *J Neuropathol Exp Neurol* 2002; **61**: 268–274.
19. Iwasaki Y, Yoshida M, Hattori M, Hashizume Y, Sobue G. Widespread spinal cord involvement in corticobasal degeneration. *Acta Neuropathol (Berl)* 2005; **109**: 632–638.
20. Litvan I, Agid Y, Calne D *et al.* Clinical research criteria for the diagnosis of progressive supranuclear palsy (Steel–Richardson–Olszewski syndrome): report of

Richardson–Olszewski syndrome (progressive supranuclear palsy). *Neurology* 1994; **44**: 2015–2019.

the NINDS-SPSP international workshop. *Neurology* 1996; **47**: 1–9.

21. Terao S, Sobue G, Hashizume Y, Mitsuma T, Takahashi A. Disease-specific patterns of neuronal loss in the spinal ventral horn in amyotrophic lateral sclerosis, multiple system atrophy and X-linked recessive bulbospinal neuronopathy, with special reference to the loss of small neurons in the intermediate zone. *J Neurol* 1994; **241**: 196–203.

22. Kato S, Hirano A, Llena JF. Immunohistochemical, ultrastructural and immunoelectron microscopic studies of spinal cord neurofibrillary tangles in progressive supranuclear palsy. *Neuropathol Appl Neurobiol* 1992; **18**: 531–538.

23. Murakami N, Yoshida M, Aiba I, Hashizume Y. *Neuropathological characteristics of anterolateral funiculus of spinal cord of progressive supranuclear palsy (PSP) – in comparison with amyotrophic lateral sclerosis.*

Annual report of the research committee of CNS degenerative disease, Ministry of Health and Welfare of Japan, 1995; 210–213 (in Japanese with English Abstract).

24. Rexed B. A cytoarchitectonic atlas of the spinal cord in the cat. *J Comp Neurol* 1954; **100**: 297–351.

25. Iwatsubo T, Hasegawa M, Ihara Y. Neuronal and glial tau-positive inclusions in diverse neurologic diseases share common phosphorylation characteristic. *Acta Neuropathol (Berl)* 1994; **88**: 129–136.

26. Andre P. Spinal cord: regional anatomy and internal structure. In: Andre P, ed. *Carpenter's Human Neuroanatomy*, 9th edn. Baltimore, MD: Williams & Wilkins, 1996; 325–367.

27. Kuypers HG. A new look at the organization of the motor system. *Prog Brain Res* 1982; **57**: 381–403.

28. Kandel ER, Schwarz JH, Jessell TM. *Principles of Neural Science*, 3rd edn. Amsterdam: Elsevier, 1991.

Clinical Research Paper

Dobutamine stress test unmasks cardiac sympathetic denervation in Parkinson's disease

Tomohiko Nakamura [a], Masaaki Hirayama [a], Hiroki Ito [a], Motoko Takamori [a], Kensuke Hamada [b], Shigeo Takeuchi [b], Hirohisa Watanabe [a], Yasuo Koike [c], Gen Sobue [a,*]

[a] Department of Neurology, Nagoya University Graduate School of Medicine, 65 Tsurumai-cho, Showa-ku, Nagoya 466-8550, Japan
[b] Department of Neurology, Aichi-ken Saiseikai Hospital, 1-1-18 Sako, Nishi-ku, Nagoya 451-0052, Japan
[c] Department of Health Science, Nagoya University Graduate School of Medicine, 1-1-20 Daikominami, Higashi-ku, Nagoya 461-8673, Japan

Abstract

Objective: Cardiac uptake of [^{123}I]metaiodobenzyl guanidine (MIBG) is reduced in patients with Parkinson's disease (PD). However, the cardiac sympathetic abnormality associated with this reduction is unclear. To unmask this abnormality in PD patients we examined the functional consequences of cardiac beta-receptor activation.

Methods: Cardiovascular responses to stepwise administration of the beta1-receptor agonist, dobutamine (DOB), were assessed in 25 PD patients and 12 age-matched controls. Changes in blood pressure were compared to determine the optimal dose at which to detect denervation supersensitivity, and cardiac contractility was measured by DOB echocardiography, based on peak aortic flow velocity. The relations of these cardiovascular responses to the ratio of MIBG uptake into the heart vs. that into the mediastinum (H/M ratio) were analyzed.

Results: At 4 µg/kg/min DOB, systolic blood pressure increased more in PD patients than in controls (PD, 17.5 ± 12.3 mm Hg; control, 7.2 ± 6.2 mm Hg, $p<0.01$), suggesting the presence of denervation supersensitivity. At this DOB dose cardiac contractility also increased more in PD than in controls (PD, $39.0 \pm 15.7\%$; control, $23.5 \pm 5.2\%$, $p<0.005$) and this hyperdynamic response was significantly correlated with reduced H/M ratios (early: $r=-0.63$, $p<0.01$, delayed: $r=-0.66$, $p<0.01$).

Conclusion: Low-dose DOB unmasks cardiac sympathetic denervation in PD patients, and decreased MIBG uptake indicates the presence of denervation supersensitivity within the heart, resulting in hyperdynamic cardiac contractility in response to a beta 1-stress condition.
© 2007 Elsevier B.V. All rights reserved.

Keywords: Parkinson's disease; Dobutamine; Denervation supersensitivity; Cardiac sympathetic denervation; Dobutamine echocardiography; MIBG; Cardiac contractility

1. Introduction

Since Hakusui first demonstrated cardiac sympathetic nerve damage in patients with Parkinson's disease (PD) by decreased cardiac [^{123}I]metaiodobenzyl guanidine (MIBG) uptake [1], a large number of studies have documented this phenomenon [2–4]. Uptake of MIBG reflects myocardial sympathetic nerve function [5]. Histological assessment of the sympathetic nerve axon population innervating cardiac

muscle is also markedly decreased in PD patients and is considered to account for the decrease in MIBG uptake [6,7]. Severe abnormal MIBG findings in peripheral vessels were also found in PD with autonomic failure [8]. However, the cardiac sympathetic abnormality correlated to reduced MIBG uptake in PD patients has not been clarified. Echocardiography has demonstrated normal ventricular systolic function under resting conditions in PD patients [9].

Cardiovascular responses to sympathomimetic agents have been anecdotally described to be exaggerated in PD patients [10,11] but it is unclear whether these responses are due to impaired cardiac sympathetic nerve function or other

---

peripheral/central autonomic system abnormalities. Dobutamine (DOB) is a synthetic sympathomimetic amine that directly stimulates beta-adrenergic receptors, especially beta1-receptors [12,13]. In normal subjects, infusion of DOB in doses up to 10 μg/kg/min increases cardiac output and heart rate (HR) but has little effect on blood pressure (BP) [13,14]. DOB is commonly used in the stress test to diagnose ischemic heart disease [15,16]. Specifically, low-dose DOB has been used, because it is safe and convenient to administer, to identify viable myocardial impairment [17,18].

In PD patients, various degrees of primary chronic autonomic failure are seen and some patients with orthostatic hypotension display evidence of cardiac sympathetic denervation [19]. Thus, it is clinically important to clarify how this cardiac denervation correlates with the decreased MIBG uptake that is commonly seen in PD patients. The purpose of this study was to assess the cardiovascular response of beta1-adrenergic receptors using low-dose DOB to detect cardiac denervation supersensitivity and unmask the cardiac abnormality associated with decreased MIBG uptake in patients with PD. Echocardiography was performed to evaluate the cardiac response to DOB and verify the association between this response and the degree of cardiac MIBG uptake.

2. Subjects and methods

2.1. Subjects

We included 25 patients with PD (10 men, 15 women) who were referred to the Nagoya University Hospital. PD was diagnosed according to the United Kingdom Parkinson's Disease Society Brain Bank Clinical Diagnosis Criteria [20]. All patients underwent precise neurological examinations and brain MRIs to exclude diagnoses other than PD. In all cases, no obvious heart disease, including experience of anginal pain, or diabetes mellitus was detected and electrocardiographs were all normal. The mean patient age was 65.5 ± 8.1 and the mean duration since the onset of symptoms was 4.8 ± 3.7 years (range: 1 to 12 years; Table 1). The control subjects were normal healthy volunteers (5 men, 7 women, 61.1 ± 14.0 years old) with no history of heart disease, diabetes mellitus, or intracranial disease and no obvious abnormalities observed on physical examination. Orthostatic hypotension was absent during head-up tilt testing in the control group. Informed consent was obtained from all participants and the protocol of the study was approved by the ethics committee of Nagoya University Graduate School of Medicine.

2.2. DOB infusion test

Patients abstained from eating and the use of anti-parkinsonian drugs on the morning of testing. No patient took other drugs that might influence BP responses, such as

Table 1
Clinical characteristics

	PD (n=25)	Control (n=12)	p value
Age (years)	65.5 (8.1)	61.1 (14.0)	N.S.
Gender (M/F)	10/15	5/7	N.S.
Disease duration (years)	4.8 (3.7)		
Hoehn and Yahr stages	I:3; II:6; III:8; IV:8		
Levodopa (mg/day)	254.8 (190.4)		

Values are expressed as mean (±SD). PD=Parkinson's disease; N.S.=not significant.

midodorine or droxidopa. The subjects were tested in the supine position. After resting for at least 5 min, DOB (2 μg/kg/min; 0.5 ml/min) was administered by continuous intravenous infusion via a brachial venous cannula using a constant infusion pump. After 5 min the infusion was increased to 4 μg/kg/min and continued for another 5 min until: (1) the systolic BP (SBP) was > 170 mm Hg or the SBP increase was >40 mm Hg, or (2) the HR > 100/min, or (3) there was an increase in the frequency of arrhythmias, or (4) the development of untoward side effects. BP and HR were recorded every minute with an automated sphygmomanometer (BP-508, Nippon Colin, Tokyo, Japan), designed for autonomic studies, placed on the upper arm opposite to that used for the DOB infusion. The electrocardiogram was monitored continuously throughout the procedure.

2.3. Echocardiographic examination

DOB echocardiography of Doppler examinations were performed using a Hewlett Packard Sonos 1500 ultrasound system (Andover, MA) with 1.9 MHz (Pedoff) transducers. The entire exam was performed by a single investigator who did not know the results of the MIBG scintigraphy. The aortic flow velocity (AFV) waveform was acquired by continuous-wave Doppler from the supraclavicular fossa and angled toward the ascending aorta. Peak AFV was used to evaluate changes in cardiac contractility [21]. Monitoring of the aortic flow wave using echocardiography was performed 3 min after each incremental DOB infusion. When sharp, well-defined velocity waveforms were seen on the monitor and maximal pitch was heard through the integral loudspeaker, a 5-s recording was "frozen" on-screen and measurements were made directly from the monitor using a built-in light pen system with dedicated software.

2.4. MIBG scintigraphy

MIBG (111 mBq) was injected intravenously into each subject. The early image of cardiac uptake was obtained 15 min later and the delayed image was obtained after 3 or 4 h. Regions of interest included the whole heart and mediastinum in the anterior projection. The ratio of MIBG uptake by the heart to that in the mediastinum (H/M ratio)

Table 2
Cardiovascular response to DOB

	Baseline	DOB dosage	
		2 μg/kg/min	4 μg/kg/min
PD (n=25)			
SBP (mm Hg)	122.1 (13.8)	125.3 (16.9)*	139.6 (21.3)****
DBP (mm Hg)	69.6 (10.4)	69.9 (11.9)	72.9 (12.8)
HR (bpm)	68.9 (10.8)	67.9 (11.4)	72.4 (13.4)**
Controls (n=12)			
SBP (mm Hg)	121.4 (17.8)	123.7 (18.4)	128.6 (18.5)**
DBP (mm Hg)	70.2 (9.9)	68.6 (10.0)	67.4 (8.4)
HR (bpm)	63.7 (8.3)	63.7 (9.8)	68.0 (9.2)***

Values are expressed as mean (±SD). DOB=dobutamine; SBP=systolic blood pressure; DBP=diastolic blood pressure; HR=heart rate; bpm=beats per minute. *$p<0.05$ vs. baseline; **$p<0.01$ vs. baseline; ***$p<0.005$ vs. baseline; and ****$p<0.0001$ vs. baseline.

was calculated, and ratios from early and delayed images were evaluated.

2.5. Data analysis and statistics

Data are expressed as means (±SD). For evaluating the pharmacokinetic actions of DOB, the average values for BP and HR during the last 3 min of infusion were used for analysis. However, if the infusion was stopped in the middle of the protocol, then data from just before discontinuing the infusion were used for analysis. Supersensitive responses for the hemodynamic changes were defined as changes greater than 2 standard deviations from the mean. Tables of fre-

quency data were examined using Fisher's exact probability test. Individual data were analyzed using the Mann–Whitney's U test between groups and by Wilcoxon's signed rank test within the groups. Relationships with the H/M ratio were analyzed using Spearman's correlation coefficient. Calculations were performed using the statistical software package StatView (Abacus Concepts, Berkeley, CA). The level of significance was defined at $p<0.05$.

3. Results

3.1. Appropriate dose of DOB to detect a supersensitive response in PD patients

There were no significant differences in baseline cardiovascular measurements between the PD patients and the control subjects (Table 2). During the 2 μg/kg/min DOB infusion, the mean SBP increased significantly in the PD subjects but not in control subjects; no significant changes in mean diastolic BP (DBP) or HR changes were observed in either group. During the 4 μg/kg/min DOB infusion, mean SBP increased another 14.3 mm Hg in the PD subjects but the increase was only slight in control subjects. No significant DBP change was seen in either group at this dose. HR increased in both groups.

All control subjects completed the entire procedure. All PD patients also completed the procedure, however, six (24%) had met our withdrawal criteria by the end of the 4 μg/kg/min dose of DOB (1 with SBP >170 mm Hg, 1 with SBP
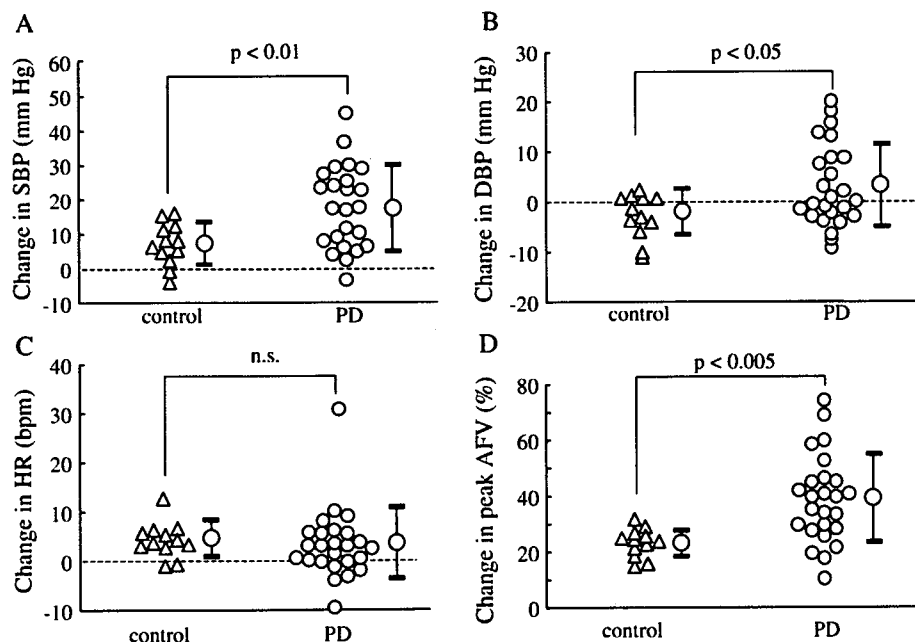

Fig. 1. Changes in SBP, DBP, HR, and peak AFV after infusion of 4 μg/kg/min DOB in controls and PD patients. (A) The mean change in SBP is significantly greater in the PD group than in the control group. (B) There was also a significant difference in the DBP change between the PD and control groups. (C) No difference was seen in the HR change between the groups. (D) The mean percentage change in peak AFV was significantly larger in the PD group than in the control group. SBP: systolic blood pressure, DBP: diastolic blood pressure, HR: heart rate, DOB: dobutamine, AFV: aortic flow velocity, PD: Parkinson's disease. n.s.=not significant.